Flow-Induced Particulate Separations

Brian W. Roberts and W. L. Olbricht
School of Chemical and Biomolecular Engineering,
Cornell University, Ithaca, NY 14853

Separating particles from the liquid in which they are suspended is often an important step in processing multiphase materials such as suspensions and emulsions. We describe a new method to separate neutrally buoyant particles from viscous liquids. The method is based on the low Reynolds number motion of freely-suspended particles at bifurcations — points where a tube or channel splits into multiple tubes. We show experimentally that the partitioning of particles at a bifurcation differs from the partitioning of the suspending fluid. The effects of particle size, particle volume fraction, and shape of the bifurcation on particle partitioning are examined. Furthermore, we demonstrate that when tubes and bifurcations are arranged in certain ways, the particles can take preferential paths through the network and can be separated from the liquid in which they are suspended. The data show that the particle separation can be enhanced in relatively simple networks consisting of just a few interconnected channels.

Introduction

Separating solid particles from the liquid in which they are suspended is an essential operation in many processes of technological and biological importance. When the particles are neutrally buoyant in the suspending liquid, removing them poses special challenges because sedimentation and centrifugation are ineffective. Filtration is an alternative for these cases, but many filtration methods have practical difficulties that reduce their efficiency and limit their applicability. These difficulties include a concentration polarization near the membrane, the buildup of retained particles in a filter cake, solute rejection, and large pressure drops across the membrane that increase in time. Furthermore, most filtration methods are inherently batch processes; eventually, retained particles must be purged from the filter or the filter must be replaced.

New methods of removing particles from viscous liquids could prove useful, especially if they could be incorporated as continuous operations in manufacturing processes. Since many suspensions are processed under flowing conditions, it may be convenient to use characteristics of the flow to separate the particles from the liquid. However, methods of flow-induced particle separation are rare.

Poflee et al. (1997,1998) exploited the inertial migration of particles in tube flow to separate particles from liquids. When the Reynolds number is sufficiently large, small particles near the tube wall migrate across streamlines and congregate in the central region of the tube. Far downstream, particle-free fluid near the tube wall can be removed, leaving a concentrated suspension of particles that flows down the main tube. However, inertial migration is a slow process, because the migration rate scales with the Reynolds number based on the particle diameter. The particle Reynolds number is smaller than the tube Reynolds number, and it cannot be made arbitrarily large by increasing the flow rate, because the flow must remain laminar. Consequently, the suspension must flow through a relatively long tube before the particles become concentrated in the central part of the tube.

Separations that are driven by inertial effects are ineffective for very viscous liquids, for slow flows, or for flows in small channels, because the Reynolds number in these cases is too small to drive the lateral migration. Many of the miniaturized devices that have been developed recently to carry out novel, small-scale chemical processing and analysis use microfluidics to transport liquids in micron-sized channels and networks of such channels. Practitioners of microfluidics point out that the flow in such devices is laminar, which has important implications for mixing and mass transfer. Indeed, in many microfluidic applications, the Reynolds number is so small that not only is the flow laminar, but it is also in the creeping flow regime, owing to the small channel dimensions. This distinction may not be important for the flow of a pure liquid in a straight channel, but it is important for multiphase

Correspondence concerning this article should be addressed to W. L. Olbricht.

systems such as suspensions and emulsions. When the Reynolds number based on particle size is less than unity, the motion of freely suspended particles is determined by viscous and pressure forces, and inertially driven migration across streamlines is insignificant. Interactions among particles in concentrated suspensions can induce particle migration across streamlines in low Reynolds number channel flow, but the slow migration rate requires long channels before a significant variation in particle concentration is observed (Lyon and Leal, 1998). To extend microfluidic processing to multiphase systems, it would be useful to have a flow-induced particle separation method that is effective and efficient in the small Reynolds number limit.

This article describes a new particulate separation process based on the low Reynolds number flow of suspensions through channels that split to form multiple channels. The simplest example of such a channel is a straight tube that splits into two tubes at a junction called a bifurcation. When a suspension flows through a tube containing a bifurcation, the partitioning of particles between the two downstream branches differs from the partitioning of total volume (particles + suspending fluid) between the downstream branches (Johnson, 1971; Fung, 1973; Papenfuss and Gaehtgens, 1979; Klitzman and Johnson, 1982; Dellimore et al., 1983; Fenton et al., 1985; Pries et al., 1989; Ditchfield and Olbricht, 1996). The effect is purely hydrodynamic, and it can be demonstrated by solving the equations of motion for low Reynolds number flow, although this is a formidable problem (Audet and Olbricht, 1987; Audet 1987, Poulou, 1995). The only restrictions are that the Reynolds number is small and Brownian motion is not important.

It is convenient to identify two features that explain qualitatively the partitioning of particles at bifurcations. First, the radial distribution of particles is nonuniform in the tube upstream of a bifurcation, because particle centers are excluded from a layer adjacent to the tube wall whose thickness is the particle radius. Second, the velocity of a freely suspended particle differs in magnitude and direction from the velocity of the surrounding suspending fluid owing to hydrodynamic interactions between the particle and the channel walls. When the particle size is comparable to the channel diameter, both effects are important, and the difference between the particle flux and volume flux entering each branch can be substantial.

Physiologists who study the motion of blood cells in the microcirculation observe this phenomenon routinely. They have long been interested in the distribution of blood cells in capillary networks, which has led to numerous studies of red blood cell partitioning at capillary bifurcations *in vitro* and *in vivo*. Much of this work has been reviewed by Ditchfield and Olbricht (1996). A typical experiment is to measure flow rates in the downstream branches and count the number of cells that enter each branch. When the cell size is comparable to the vessel diameter, in many instances the particles "favor" the downstream branch receiving the greater volumetric flow rate. If the flow rate in one of the branches is made sufficiently large, all of the cells enter that branch and only plasma enters the other branch.

We have conducted a series of experiments to examine flow through bifurcations and the separation of particles for a well-defined model system—a suspension of neutrally buoyant rigid spheres in a viscous liquid—whose material properties are known precisely. We use the results for particle motion at a single bifurcation to suggest possible designs of a practical device to separate particles. We show results for a simple prototype that consists of multiple bifurcations in series arranged in a particular way that exploits changes in the radial distribution of particles downstream of a bifurcation. We also examine the effects of various material parameters on the efficiency of the separation. We consider cases when the particles are sufficiently large and the suspending fluid is sufficiently viscous that Brownian motion is unimportant. Furthermore, nonhydrodynamic forces between the particles and the channel walls, such as electrostatic or van der Waal's attraction, are negligible. Under these conditions, the motion and partitioning of particles at bifurcations are determined completely by hydrodynamic forces.

Experimental

Apparatus

The experiment examines the motion of particles that are freely suspended in low Reynolds number flow through a single bifurcation or, in some cases, through a series of bifurcations. Each bifurcation consists of an inlet tube that splits to form two outlet tubes. The axes of the inlet and outlet tubes lie in the same plane. Figure 1a–1c shows typical bifurcations and the parameters that define the bifurcation geometry, namely, the diameters of the channels D_0, D_1, and D_2, and the angles between each outlet channel and the inlet channel θ_1 and θ_2. Three bifurcation geometries were examined: a Y-shaped bifurcation with $\theta_1 = \theta_2 = 45°$, a T-shaped bifurcation with $\theta_1 = 0°$ and $\theta_2 = 90°$, and an oblique bifurcation with $\theta_1 = 0°$ and $\theta_2 = 135°$.

Each bifurcation was constructed from a 19-mm-thick poly(methyl-methacrylate) block by drilling holes into the block to produce the geometries shown in Figure 1. The inlet tube and the outlet tubes had circular cross-sections with equal diameters of 1 mm. The entrance of the inlet tube and the exits of the two outlet tubes were tapered at 30° to provide gradual transitions between the supply tubing and the bifurcation block. The lengths of the two outlet tubes were identical and were more than 10 tube diameters in every case. Similarly, the length of the inlet tube was more than 10 tube diameters. The bifurcation block was mounted horizontally under a CCD camera that was connected to a video recorder and timer. Particle motions at the bifurcation were examined from the video recordings after the experiment.

Figure 2 shows the entire apparatus. The suspension was loaded into a 20-mL glass syringe, which, in turn, was fitted into a Sage syringe pump. The suspension flowed out of the syringe into a section of Tygon tubing that had an inner diameter of 3.2 mm. The other end of the Tygon tubing was connected to the entrance of the inlet tube of the bifurcation. Identical Tygon tubing was connected at the exit of each outlet tube to remove fluid from the bifurcation block and transport it to waste reservoirs. Flow rates in the two downstream branches were regulated with needle valves downstream of the waste reservoirs. To prevent particles from clogging these valves, each waste reservoir contained an in-line trap that retained the particles. Flow rates were measured by timing the

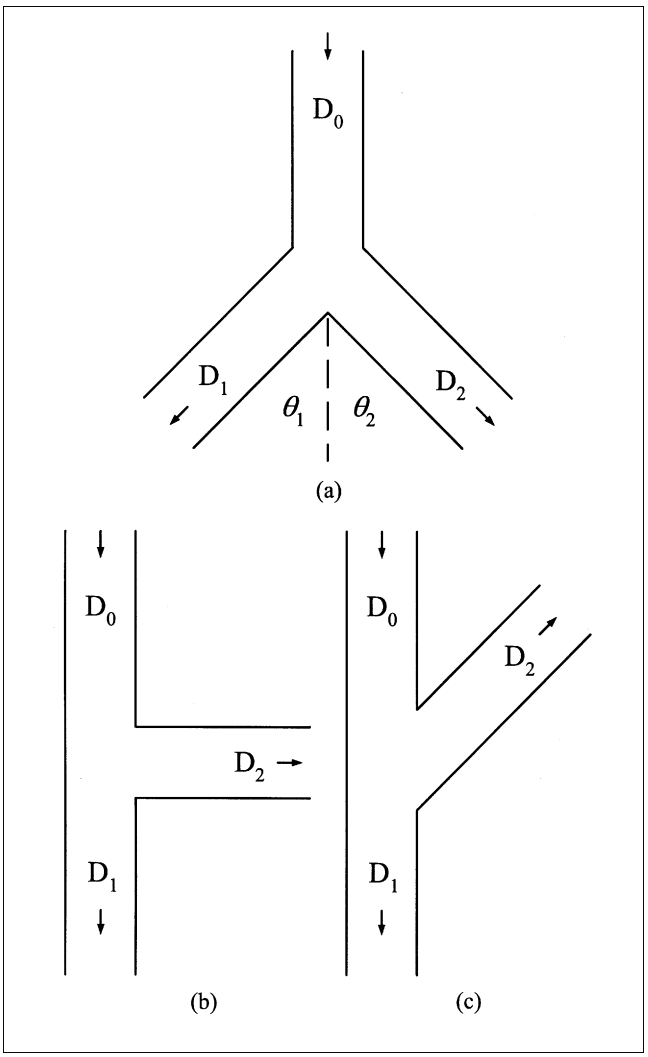

Figure 1. Three single bifurcations studied in the experiment.

(a) Y-shaped bifurcation with $\theta_1 = \theta_2 = 45°$; (b) T-shaped bifurcation with $\theta_1 = 0°$ and $\theta_2 = 90°$; (c) oblique bifurcation with $\theta_1 = 0°$ and $\theta_2 = 135°$, $D_0 = D_1 = D_2$ in all cases.

effluent from each downstream branch. Measurements during the experiments showed that the flow rate in each downstream branch did not vary significantly during the course of an experiment.

To study the effect of multiple bifurcations, the bifurcation block shown in Figure 3 was used. In this case, a single inlet tube branches into two downstream tubes. About ten diameters downstream of the first bifurcation, each downstream tube branches again into two tubes. Two numbers are used to designate each segment of the flow system, as shown in Figure 3. The geometry of the first bifurcation is Y-shaped, corresponding to the geometry shown in Figure 1a, but the two downstream bifurcations are oblique, corresponding to the geometry shown in Figure 1c.

Materials

The suspensions were composed of rigid polystyrene spheres in a viscous liquid. The spheres were certified particle standards from the Duke Scientific Corporation (www.dukescientific.com). Two nearly monodisperse suspensions were used with mean sphere diameters of 773 ± 15 μm (Duke catalog #4375A) and 497 ± 10 μm (Duke catalog

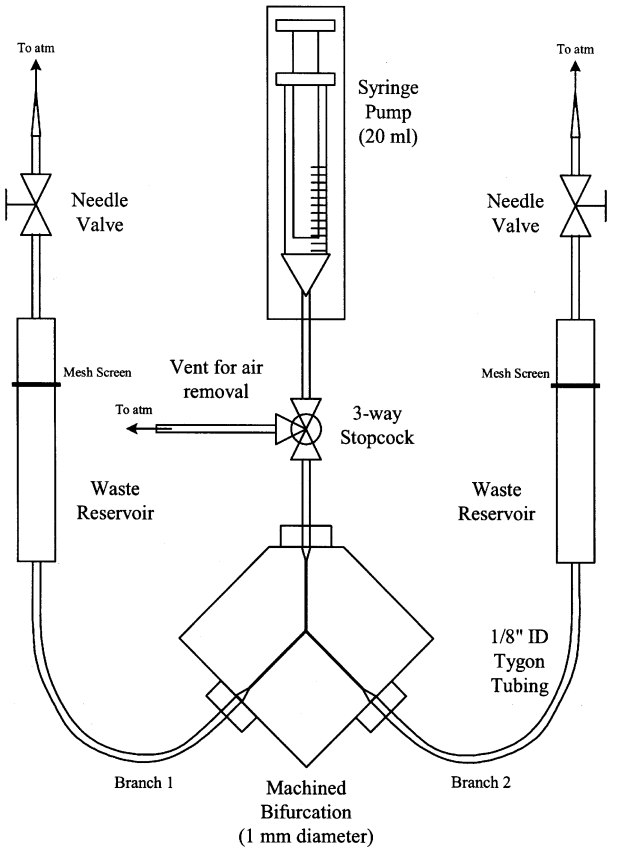

Figure 2. The apparatus.

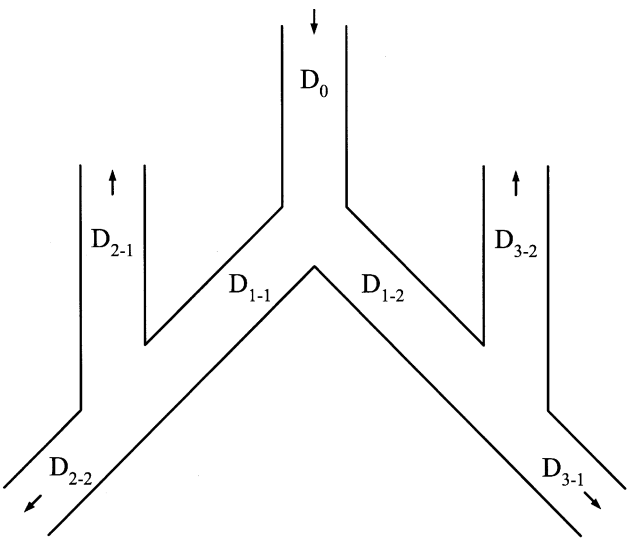

Figure 3. System of multiple bifurcations containing one inlet and four outlets; each fluid path through the system contains two bifurcations in series.

#4350A). The dimensionless particle size λ is defined as the ratio of the particle diameter to the channel diameter. Since the diameter of all bifurcation branches was 1 mm, the two suspensions had dimensionless particle sizes λ of 0.50 and 0.77. The suspending fluid was 65% Triton X-100 (VWR Catalog #EM-9440), a nonionic surfactant and 35% water. The density of the Triton X-100 was 1.07 g/cm^3, and the density of the Triton X-100–water mixture was 1.05 g/cm^3, which closely matched the density of the spheres. The viscosity of the suspending fluid was 1.1 Pa-s, which produced a maximum Reynolds number based on the tube diameter of 9×10^{-3}. Two values of the particle volume fraction ϕ were studied: 0.02 and 0.06. Although these values may seem small, previous studies (Ditchfield and Olbricht, 1996) showed that interactions among the particles can influence particle trajectories at bifurcations for surprisingly small values of ϕ.

Procedure

The suspension was well mixed and loaded into the syringe. The volumetric flow rates in the downstream branches are denoted by Q_1 and Q_2. For the T-shaped and oblique bifurcations, the subscript "1" refers to the downstream branch that is colinear with the inlet branch. For the Y-shaped bifurcation, there is no distinction between the two downstream branches owing to the symmetry of the bifurcation shape. By mass balance, the flow rate in the inlet branch Q_T is simply $Q_1 + Q_2$. For each bifurcation geometry, for each dimensionless particle size, and for each value of the particle volume fraction, several runs were made for different combinations of Q_1 and Q_2. Values were chosen so that the fraction of the flow that entered branch 1, Q_1/Q_T, varied from almost zero to almost unity. After each experimental run, the video recording was reviewed to determine N_1 and N_2, the numbers of particles that entered branches 1 and 2, respectively. The total number of particles that flowed through the bifurcation, N_T, is simply $N_1 + N_2$. The experiments were run with a sufficiently large number of particles that the fractions of particles entering each branch, N_1/N_T and N_2/N_T, did not depend on the number of particles used in the experiment. The video recording was also used to examine particle trajectories in the vicinity of the bifurcation.

3 Results

It is convenient to report data for the particle distribution at a bifurcation in terms of N_1/N_T, the fraction of particles that entered branch 1, as a function Q_1/Q_T, the fraction of total volume (suspending fluid + particles) that entered that branch. By mass balance, $N_2/N_T = 1 - N_1/N_T$ and $Q_2/Q_T = 1 - Q_1/Q_T$.

Results for the Y-shaped bifurcation are shown in Figure 4 for three combinations of particle size λ and particle volume fraction ϕ. The data show that for all three cases, the particles favor the branch receiving the greater flow rate. The diagonal line in Figure 4 corresponds to the hypothetical case where the particles and fluid distribute identically between the two downstream branches of the bifurcation. Therefore, the deviation of the data from the diagonal line is a quantitative measure of the particle separation effectiveness over the range of values of Q_1/Q_T. Comparing the three sets of data

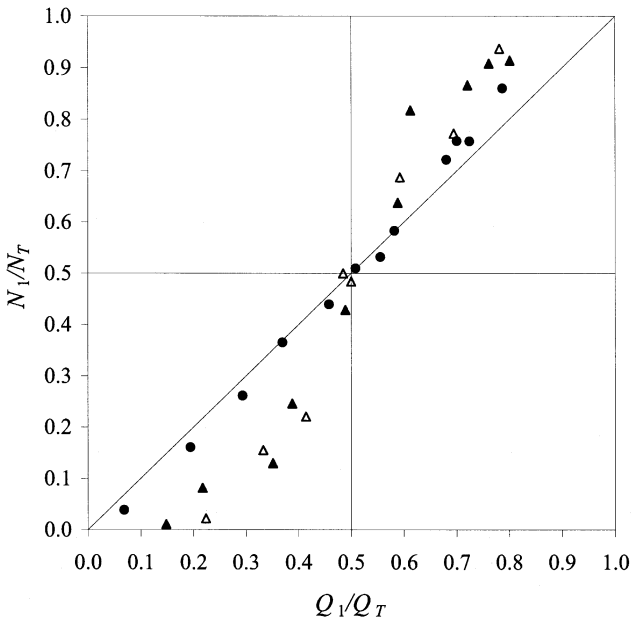

Figure 4. Fraction of particles entering branch 1 as a function of the fraction of total volume entering that branch for the Y-shaped bifurcation in Figure 1(a).

(▲) $\lambda = 0.77$ and $\phi = 0.02$; (△) $\lambda = 0.77$ and $\phi = 0.06$; (●) $\lambda = 0.5$ and $\phi = 0.02$.

shows that the particle separation is more effective for larger particles and for smaller volume fractions. The case $\lambda = 0.5$ and $\phi = 0.06$ produced data very close to the diagonal line, which indicates a negligible separation; the data for this case were omitted from the figure. Owing to the symmetry of the Y-shaped bifurcation geometry, each set of data in Figure 4 is symmetric about the point $Q_1/Q_T = 0.5$.

The data show that if the fraction of the flow in branch 1 exceeds some critical value, say $(Q_1/Q_T)^*$, then all of the particles enter branch 1. The value of $(Q_1/Q_T)^*$ decreases with increasing particle size λ and decreasing particle volume fraction ϕ. As expected from the symmetry of the bifurcation, if the value of Q_1/Q_T is made sufficiently small, then all of the particles enter branch 2.

Results for the T-shaped bifurcation in Figure 1b are shown in Figure 5 for the same parameter combinations as in Figure 4. The symmetry of the data about the point (0.5, 0.5) is broken, because the shape of the T-bifurcation geometry is not symmetric. When the majority of the flow enters the side branch (branch 2), which corresponds to $Q_1/Q_T < 0.5$, the particles favor the side branch, but the deviation from the diagonal line is relatively small. When the majority of the flow enters the straight branch (branch 1), which corresponds to $Q_1/Q_T > 0.5$, the particles strongly favor branch 1, and the difference between the data and the diagonal line is appreciable. Furthermore, the critical value $(Q_1/Q_T)^*$, for which all of the particles enter branch 1, is about 0.7 for $\lambda = 0.77$ and $\phi = 0.02$. The separation is more effective for the larger particles, which was observed also for the Y-shaped bifurcation. However, there is a measurable deviation from the diagonal line for $\lambda = 0.5$ for the T-bifurcation, and when Q_1/Q_T

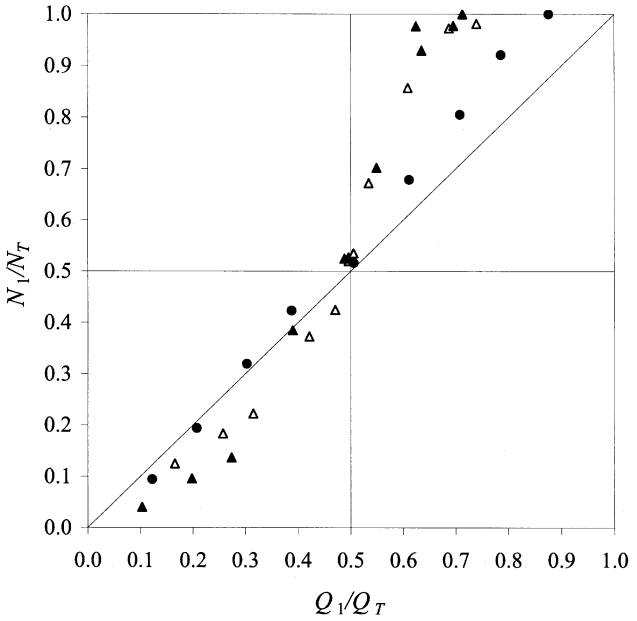

Figure 5. Fraction of particles entering branch 1 as a function of the fraction of total volume entering that branch for the T-shaped bifurcation in Figure 1(b).

(▲) $\lambda = 0.77$ and $\phi = 0.02$; (△) $\lambda = 0.77$ and $\phi = 0.06$; (●) $\lambda = 0.5$ and $\phi = 0.02$.

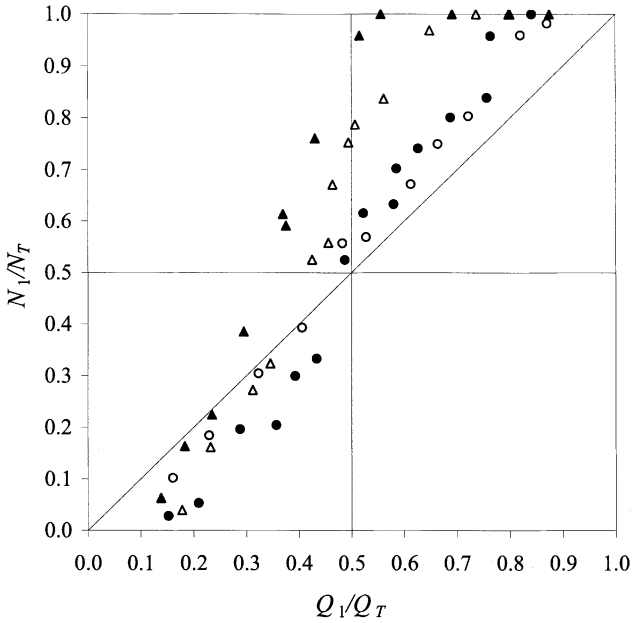

Figure 6. Fraction of particles entering branch 1 as a function of the fraction of total volume entering that branch for the oblique bifurcation in Figure 1(c).

(▲) $\lambda = 0.77$ and $\phi = 0.02$; (△) $\lambda = 0.77$ and $\phi = 0.06$; (●) $\lambda = 0.5$ and $\phi = 0.02$; (○) $\lambda = 0.5$ and $\phi = 0.06$.

exceeds 0.87, all of the particles enter branch 1. The data for the T-bifurcation appear less sensitive to the value of particle volume fraction ϕ than the data for the Y-bifurcation. For $\lambda = 0.77$ the curves for $\phi = 0.02$ and 0.06 nearly coincide.

Results for the oblique bifurcation illustrated in Figure 1c are shown in Figure 6 for the same parameter combinations and for the additional case of $\lambda = 0.5$ and $\phi = 0.06$. For the three cases that were covered in the previous geometries, data for the oblique bifurcation resemble qualitatively the data for the T-shaped bifurcation. However, the deviation from the diagonal line is considerably greater in the oblique bifurcation, indicating a greater separation effectiveness. The larger particles ($\lambda = 0.77$) strongly favor the straight branch for $Q_1/Q_T > 0.3$ (for $\phi = 0.02$) and for $Q_1/Q_T > 0.4$ (for $\phi = 0.06$). The smaller particles ($\lambda = 0.5$) also favor the straight branch, although the separation effectiveness is smaller than that for the larger particles. The critical value $(Q_1/Q_T)^*$, when all of the particles enter branch 1, is about 0.55 for $\lambda = 0.77$ and $\phi = 0.02$, which is smaller than the corresponding values for the T-shaped and Y-shaped bifurcation. Table 1 lists values of the critical flow split $(Q_1/Q_T)^*$ for all cases covered in the experiment.

Preliminary experiments showed that small imperfections in the machining of the bifurcations can affect the measured values of the particle fractions entering each branch. Although care was taken in machining the bifurcations, small variations in the branch angles and small imperfections in the contour of the channels at the junctions are difficult to avoid. Such imperfections can influence particle trajectories, and they could affect which branch certain particles enter downstream of the bifurcation. A relatively small number of altered trajectories could account for the observed scatter in the data and explain why, for example, the data in Figure 4 are not perfectly symmetric about the point (0.5, 0.5). Also, we used gradual tapers from the syringe to the entrance of the inlet channel to ensure a uniform distribution of particles across the radius of the inlet channel. On several occasions we measured the radial positions of particles passing a fixed location in the inlet channel and found no variations in the particle frequency with radial position, except in the excluded region adjacent to the tube wall. However, we could not monitor the particles in the inlet channel during an experiment; an inadvertent nonuniform distribution of particle locations in the inlet channel could affect the measured results.

Multiple Bifurcations

The results presented in the preceding section show that flow through a bifurcation results in an appreciable separation of particles over a wide range of flow splits. However, unless the value of Q_1/Q_T is either very large or very small, the separation at a single bifurcation is incomplete. It seems reasonable to ask whether the overall effectiveness of the separation could be improved by passing a suspension through

Table 1. Values of $(Q_1/Q_T)^*$ for Single Bifurcations in Figure 1

	Bifurcation		
Parameter Values	Y-Shaped	T-shaped	Oblique
$\lambda = 0.77$, $\phi = 0.02$	0.80	0.69	0.55
$\lambda = 0.77$, $\phi = 0.06$	0.85	0.72	0.73
$\lambda = 0.50$, $\phi = 0.02$	0.97	0.87	0.84
$\lambda = 0.50$, $\phi = 0.06$	—	—	0.94

several bifurcations in series in the same way that the effectiveness of certain other separation processes is improved by using repeated stages. If so, then how should the bifurcations be arranged and how should the flow rates be regulated to achieve the optimal separation?

Before turning to those issues, we consider the flow through multiple bifurcations in series and ask whether flow through the first bifurcation influences the separation that is obtained at downstream bifurcations. To address this issue, we focus on the radial distribution of particles in the inlet channel upstream of the first bifurcation and in the channels downstream of the first bifurcation. In the absence of Brownian motion and nonhydrodynamic forces, the trajectory of a particle moving through the bifurcation depends on the particle's radial position in the inlet branch. Audet and Olbricht (1987) calculated trajectories of freely suspended particles in a two-dimensional (2-D) analog of Y- and T-shaped bifurcations. The computed trajectories show that the radial distributions of particles are not uniform in the downstream branches, even though the radial distribution of particles is uniform in the inlet branch (except for the region adjacent to the wall, where particle centers are excluded).

For example, the radial distributions of particles in the downstream branches of a Y-shaped bifurcation are skewed toward the inner walls of the Y (Audet and Olbricht, 1987). Fluid near the inner walls of the downstream branches originates near the center line of the inlet tube. The flow carries particles from the central region of the inlet tube to the inner walls of the downstream branches. However, fluid near the outer walls of the downstream branches originates near the particle-free layer of the inlet tube. Thus, fluid near the outer walls of the downstream branches is deficient in particles. These remarks pertain to a Y-shaped bifurcation, but the result holds qualitatively regardless of the bifurcation shape; the radial particle distribution is nonuniform in downstream branches of a bifurcation. The issue then becomes whether this nonuniform distribution can be exploited using successive bifurcations to improve the overall effectiveness of a separation.

Figure 3 shows a simple arrangement of bifurcations to demonstrate the effect of nonuniform radial profiles in the downstream branches. In this design, the suspension flows first through a Y-shaped bifurcation and then through an oblique bifurcation. The particles in both branches downstream of the first bifurcation reside near the inner walls. However, the oblique branch of the second bifurcation takes fluid from the vicinity of the outer walls. Therefore, fluid entering the oblique branch of the second bifurcation should be deficient in particles.

The same procedure as in the second section was followed to study particle flux in the multiple bifurcation network shown in Figure 3. However, the flows from the colinear segments of the downstream bifurcations, segments labeled 2-2 and 3-1 in Figure 3, were combined into a single stream designated as "outlet 1." Flows from the two oblique branches of the downstream bifurcations, segments 2-1 and 3-2, were combined into a single stream designated as "outlet 2." Particle fluxes for the combined streams are reported in the same way data were reported in the third section for single bifurcations.

The results for the multiple bifurcation system are shown in Figure 7. The fractional particle flux in the combined outlet 1, N_1/N_T, lies above the diagonal line for $Q_1/Q_T > 0.2$. For each combination of λ and ϕ, the deviation from the diagonal line is greater than for any of the single bifurcations alone. The particles strongly favor the colinear branches of the second bifurcations, which reflects a combination of the bifurcation geometry and the nonuniform distribution of particles caused by the first bifurcation. The differences between these results and the single bifurcation results are especially large for smaller values of Q_1/Q_T. For example, for the larger particles, the value of N_1/N_T is about 0.8 when the fractional flux into outlet 1, Q_1/Q_T, is only about 0.25. The separation is less effective for the smaller particles, but it is better than the single bifurcation results for them, too. The multiple bifurcation system gave the smallest values of the critical flow flux. Values of $(Q_1/Q_T)^*$ for the three parameter combinations are shown in Table 2.

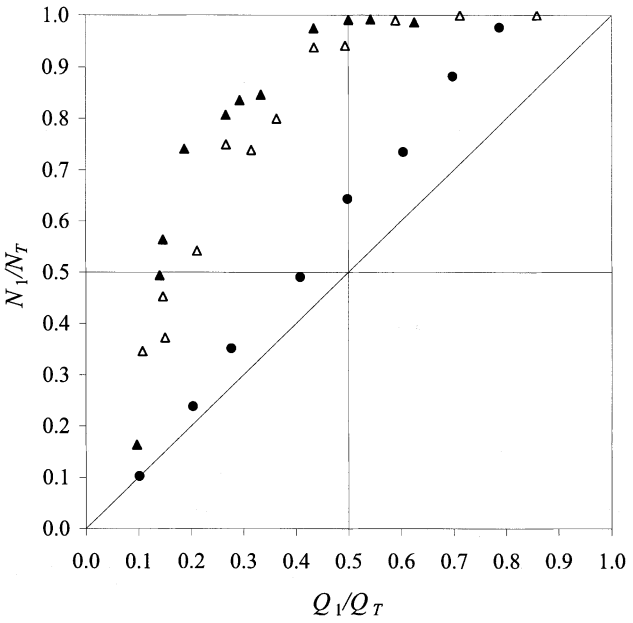

Figure 7. Fraction of particles entering combined outlet 1 as a function of the fraction of total volume entering that outlet for the multiple bifurcation system in Figure 3.

(▲) $\lambda = 0.77$ and $\phi = 0.02$; (△) $\lambda = 0.77$ and $\phi = 0.06$; (●) $\lambda = 0.5$ and $\phi = 0.02$.

Discussion

Results for the single bifurcations show that particle partitioning at a bifurcation depends strongly on the bifurcation geometry, the dimensionless particle size, and the particle volume fraction. For the Y-shaped bifurcation, the downstream branch with the greater volumetric flow rate contains

Table 2. Values of $(Q_1/Q_T)^*$ for the Multiple Bifurcation Network in Figure 3

Parameter Values	$(Q_1/Q_T)^*$
$\lambda = 0.77$, $\phi = 0.02$	0.50
$\lambda = 0.77$, $\phi = 0.06$	0.60
$\lambda = 0.50$, $\phi = 0.02$	0.81

a fraction of the particles that is larger than its fraction of the volumetric flow. The preference for the branch with the greater flow rate increases with particle size. Figure 4 suggests that in the limit $\lambda \to 1$, the sigmoidal-shaped curves may tend toward a step function where all particles move into the branch with the greater volumetric flow rate.

When the bifurcation shape is not symmetric, as in the T-shaped and the oblique bifurcations, the partitioning of particles favors the colinear branch rather than the side branch. This effect increases as the branching angle increases from 90° to 135°. Data for the oblique bifurcation show that the colinear branch may receive a majority of the particles even when it receives less than half of the volumetric flow. These results confirm, at least qualitatively, numerical simulations by Poulou (1995) that suggested geometries with oblique branches should show greater separation efficiency.

Particle–particle interactions affect the distribution of particles for surprisingly small values of the particulate volume fraction. For the small particle volume fractions in this experiment, interactions among particles in the inlet tube are infrequent. However, interactions between particles inside the bifurcation are much more common. As a particle nears the apex of a bifurcation (the wall of the junction that is opposite the inlet tube), its transitional velocity decreases (Chien et al., 1985; Ditchfield and Olbricht, 1996). Observations show that frequently the next particle upstream has time to enter the bifurcation and interact with the first particle, even though these particles were sufficiently far apart in the inlet tube that they did not interact there. For some circumstances, the interaction perturbs the trajectory of the downstream particle so that the downstream particle enters a different branch than it would have entered in the absence of the interaction. The data show that the net effect of particle–particle interactions is to diminish the effectiveness of the separation, although the magnitude of the effect depends on the bifurcation shape. These results also support numerical simulations for pairs of particles in similarly shaped bifurcations (Poulou, 1995).

Results for bifurcations in series show that the radial distribution of particles is important in determining particle partitioning in bifurcations that are downstream of other bifurcations. Because the Reynolds number is small, there is no migration of particles across streamlines in a straight capillary. When a particle enters the downstream branch of a bifurcation, it maintains the radial position that it has at the entrance of that branch. Flow through the first bifurcation establishes a nonuniform particle profile in the downstream branches that allows predominantly particle-free fluid to be removed by the second bifurcation. This effect occurs in both downstream branches regardless of the partitioning of the flow in the first bifurcation.

The data show that particle interactions also affect the separation for bifurcations in series. For most values of Q_1/Q_T, interactions among the particles diminish the separation. However, a careful examination of Figure 7 suggests that for small values of Q_1/Q_T, the separation is practically unaffected by the volume fraction. To explain this result, we examined closely the video recordings of particle trajectories at the downstream bifurcation for small values of Q_1/Q_T.

For small Q_1/Q_T, it turns out that many of the particles follow trajectories that take them close to the apex of the downstream bifurcation. Figure 8, which was reproduced from

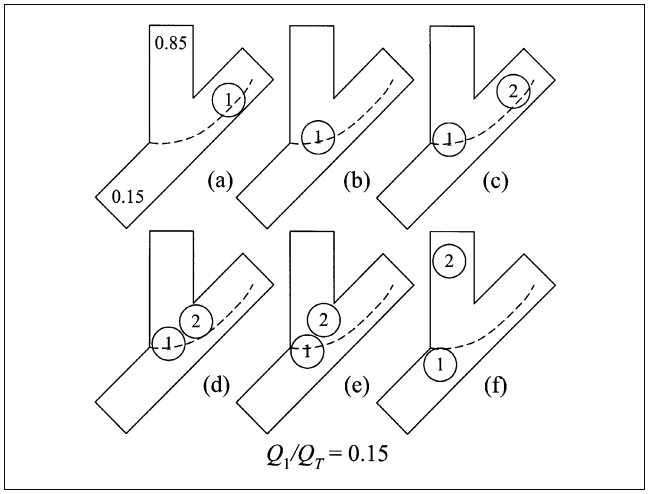

Figure 8. A series of pictures that illustrate interactions between particles at the second bifurcation in the multiple bifurcation network (Figure 3) for $\lambda = 0.77$ and $\phi = 0.06$.

(a) The first sphere near the dividing particle trajectory (dashed line); (b) the velocity of the sphere decreases near the apex of the bifurcation; (c) a second sphere approaches the bifurcation; (d) the two spheres interact in the bifurcation; (e) the interaction between spheres causes the first sphere to move into the colinear branch; (f) the result of the interaction is that the first sphere enters the colinear branch, even though it would have entered the oblique branch in the absence of the interaction with another sphere.

video recordings, illustrates a sequence of particle positions in time at one of the downstream bifurcations. The value of Q_1/Q_T in this example is 0.15, so most of the flow moves into the oblique branch, of this bifurcation. However, as a result of passing through the first bifurcation, the particles have radial positions entering the second bifurcation that are skewed toward the inner wall. The dashed line marks a hypothetical dividing trajectory for the particles. Particles whose centers are "above" the dividing trajectory in the figure move into the oblique branch, while particles whose centers are below the dividing trajectory move into the colinear branch. The center of particle 1 lies above the dividing trajectory. However, once it is inside the bifurcation, it interacts with a second particle. The interaction causes particle 1 to move into the colinear branch, although it would have moved into the oblique branch if it had not interacted with particle 2. The net effect in this case is to enhance the separation by sending more particles into the colinear branch.

Evaluating the performance of the bifurcation system as a separations device depends on the particular application, and in particular, on whether a partial or complete separation of the particles must be achieved. The quantity $(1-(Q_1/Q_T)^*)$ gives the maximum fraction of the volumetric flow rate that can be completely cleared of particles in a single pass through the device. The data in Table 2 show that the maximum fractional clearance was 0.5 for the larger particles and smaller volume fraction. However, the experimental system was designed mainly to explore effects of various parameters on particle partitioning, and there is no reason to expect that it is the optimal design for any specific application. Adding more bifurcations downstream or varying parameters that were not

varied in this experiment (such as the relative diameter of the tubes or the contours of the bifurcation walls) could improve the overall separation and increase the fractional clearance. This may be especially important for separating particles with small values of the dimensionless particle size λ, because the present results show that λ must be at least about 0.5 to achieve a significant separation in the simple devices studied here.

The results shown here could also be applied to microfluidic flow systems involving freely suspended synthetic particles or biological cells. In those cases, the design goal may not be to separate the particles from the fluid, but instead, to control which channels the particles enter as they move through the device. It might be desirable, for example, to have the particles travel along preferred paths and not enter channels that contain sensors, pumps, or other microfluidic components that could be compromised by the particles. The results shown here form the basis for rational design of microfluidic networks for multiphase systems.

The separation mechanism studied here bears a superficial similarity to earlier studies of Poflee et al. (1997, 1998) that used inertial migration in tube flow to achieve a partial separation of particles. However, the physics underlying the separations are very different in the two cases. First, inertial migration requires a Reynolds number based on the particle size that is much larger than unity. Thus, the tube Reynolds number must be as large as possible without causing turbulence. Typical values used in experiments were between 1,200 and 2,000 (Poflee et al., 1997). Second, because inertial migration is slow, the suspension must flow through a tube whose length is hundreds of diameters before the particles move away from the tube walls and a separation can be made. Third, although inertial migration requires a sufficiently large particle Reynolds number, the method can be applied to cases in which the particle is much smaller than the tube diameter. In the present work, no entrance lengths are required because the flow is in the low Reynolds number regime. The particles have negligible inertia, and their motion is dominated by viscous and pressure forces and the contours of the local bifurcation walls. A series of bifurcations can be arranged in a compact space, because the segments connecting bifurcations in series can be as short as desired. However, the data show that the particles must be comparable in size to the tube diameter to achieve an appreciable separation. Thus, the method studied here is naturally suited for microscale processing where channel diameters typically are on the scale of microns or smaller. Although the present results are limited to channels with circular cross sections, we have investigated flow through channels with rectangular cross sections, which would be a typical channel shape in microfluidic devices. Similar effects to the ones reported here are observed in rectangular channels, and this will be the subject of a future communication.

Conclusions

The results of this experiment show that flow through a network of channels and bifurcations can be a useful method of separating neutrally buoyant particles from a viscous liquid. The partitioning of particles at bifurcations, and, in turn, the effectiveness of the overall separation are affected by the particle size, the particle volume fraction, and the angles between the branches of each bifurcation. A particle clearance of 50% was easily obtained for a simple network that contained only two bifurcations in series. The results for the individual bifurcations and the simple network examined here could prove useful in designing an effective and efficient continuous separation scheme.

Acknowledgments

This material is based upon work supported by the National Science Foundation under Grant No. CTS-0074788.

Literature Cited

Audet, D. M., and W. L. Olbricht, "The Motion of Model Cells at Capillary Bifurcations," *Microvasc. Res.*, **33**, 337 (1987).

Audet, D. M., "The Numerical and Experimental Modeling of Particle Dynamics in Branching Tubes at Low Reynolds Numbers with an Application to Blood Cell Motion in Capillary Junctions," PhD Diss., Cornell Univ., Ithaca, NY, *Diss. Abstr. Int*., **48-07B**, 2040 (1987).

Chien, S., C. D. Tvetenstrand, M. A. Farrel Epstien, and G. W. Schmid-Schnbien, "Model Studies on Distributions of Blood Cells at Microvascular Bifurcations," *Amer. J. Physiol.*, **248**, H568 (1985).

Dellimore, J. W., M. J. Dunlop, and P. B. Canham, "Ratio of Cells and Plasma in Blood Flowing Past Branches in Small Plastic Channels," *Amer. J. of Physol.*, **244**, H635 (1983).

Ditchfield, R., and W. L. Olbricht, "Effects of Particle Concentration on the Partitioning of Suspensions at Small Divergent Bifurcations," *J. Biomech. Eng.*, **118**, 287 (1996).

Fenton, B. M., R. T. Carr, and G. R. Cokelet, "Nonuniform Red Blood Cell Distribution in 20 to 100 μm Bifurcations," *Microvas. Res.*, **29**, 103 (1985).

Fung, Y.-C., "Stochastic Flow in Capillary Blood Vessels," *Microvasc. Res.*, **5**, 34 (1973).

Johnson, P. C., "Red Cell Separation in the Mesenteric Capillary Network," *Amer. J. Physiol.*, **221**, 99 (1971).

Klitzman, B., and P. C. Johnson, "Capillary Network Geometry and Red Cell Distribution in Hamster Cremaster Muscle," *Amer. J. of Physiol.*, **242**, H211 (1982).

Lyon, M. K., and L. G. Leal, "An Experimental Study of the Motion of Two-Dimensional Channel Flow. Part 1. Monodisperse suspensions," *J. Fluid Mech*., **363**, 25 (1998).

Papenfuss, H. D. and P. A. L. Gaehtgens, "Effect of Bifurcations on Hematocrit Reduction in the Microcirculation. I. Fluid Dynamic Concepts of Phase Separation," *Bibl. Anat.*, **18**, 50 (1979).

Poflee, N. M., A. L. Rakow, D. S. Dandy, M. L. Chappell, and M-N. Pons, "Inertial Migration Based Concentration Factors for Suspensions of Chlorella Micro-algae in Branched Tubes," *Biorheology*, **34**, 405 (1997).

Poflee, N . M., A. L. Rakow, K. Ryan, S. Dahl, and D. S. Dandy, "Maximization of Recovery of Spirulina Platensis in a Staged Process Based on inertial Migration," *Sep. Sci. Technol*., **33**, 915 (1998).

Poulou, S. "A Numerical Model of the Partitioning of Particles at Divergent Bifurcations," PhD Diss., Cornell Univ., Ithaca NY, **55-12B**, 5463 (1995).

Pries, A. R., K. Ley, M. Claassen, and P. Gaehtgens, "Red Cell Distribution at Microvascular Bifurcations," *Microvasc. Res*., **38**, 81 (1989).

Manuscript received Sept. 11, 2002, and revision received Apr. 7, 2003.